

Article

# Modeling a Zero-Emissions Hydrogen-Powered Catamaran Ferry Using AVL Cruise-M Software

Luca Micoli \* , Tommaso Coppola, Roberta Russo and Vincenzo Sorrentino

Industrial Engineering Department, University of Naples Federico II, 80125 Napoli, Italy

\* Correspondence: luca.micoli@unina.it

**Abstract:** This work focuses on the modeling of a zero-emissions, high-speed catamaran ferry employing a full-electric propulsion system. It addresses the global emphasis on full-electric vessels to align with IMO regulations regarding ship emissions and energy efficiency improvement. Using the AVL Cruise-M software, this research verified the implementation of an onboard fuel cell power-generating system integrated with a propulsion plant, aiming to assess its dynamic performance under load variations. The catamaran was 30 m long and 10 m wide with a cruise speed of 20 knots. The power system consisted of a proton-exchange membrane fuel cell (PEM) system, with a nominal power of 1600 kW<sub>e</sub>, a battery pack with a capacity of 2 kWh, two 777 kW electric motors, and their relative balance of the plant (BoP) subsystems. The simulation results show that the battery effectively supported the PEM during the maneuvering phase, enhancing its overall performance and energy economy.

**Keywords:** zero-emissions ship; PEM application; ship performance simulation

## 1. Introduction

In the maritime sector, the urgency for sustainability seems to have risen to the forefront, propelling the exploration of alternative fuels to mitigate environmental impacts [1,2]. This drive originates from the pressing need to curtail carbon emissions and reduce the reliance on conventional fuels, actualizing a profound shift toward eco-friendly solutions. Among the alternative fuels under scrutiny—including hydrogen [3], biofuels, ammonia [4], and methanol [5]—hydrogen (H<sub>2</sub>) emerges as a particularly promising candidate, offering a transformative potential for the maritime sector [6]. Studies delving into the feasibility of integrating H<sub>2</sub> into ship operations have been ongoing since the beginning of the 21st century, exploring its application in various technologies, such as fuel cells (FCs) and internal combustion engines (ICEs), for propulsion, auxiliary power, and shore power [7]. The literature reflects diverse investigations into the viability of H<sub>2</sub>, including assessments of different FC types and methodologies for onboard H<sub>2</sub> storage and generation [8].

Notably, some research has explored the challenges associated with storing H<sub>2</sub> on board vessels, given its low volumetric energy density compared with traditional fuels, necessitating innovative storage solutions to ensure a sufficient energy supply for extended maritime voyages [9]. The storage complexities of H<sub>2</sub> encompass considerations of space, weight, and safety, which is particularly pertinent for passenger vessels. The evolving landscape of H<sub>2</sub> storage methods includes compression in gas cylinders, storage in metal hydride alloys, liquefaction in cryogenic tanks, adsorption onto high-surface-area materials, and the utilization of hydrogen carriers such as ammonia and methanol [10]. Within the context of the burgeoning hydrogen economy, the storage methods are classified into stationary and mobile applications, with a spectrum of techniques compared based on density, pressure, temperature, and cost considerations [11]. It seems that compressed gas storage methods are anticipated to dominate onboard H<sub>2</sub> storage, reflecting the advancements in fuel cell (FC) electric vehicle technology [12]. An onboard compressed H<sub>2</sub> gas system



**Citation:** Micoli, L.; Coppola, T.; Russo, R.; Sorrentino, V. Modeling a Zero-Emissions Hydrogen-Powered Catamaran Ferry Using AVL Cruise-M Software. *J. Mar. Sci. Eng.* **2024**, *12*, 770. <https://doi.org/10.3390/jmse12050770>

Academic Editor: Decheng Wan

Received: 31 March 2024

Revised: 24 April 2024

Accepted: 30 April 2024

Published: 3 May 2024



**Copyright:** © 2024 by the authors. Licensee MDPI, Basel, Switzerland. This article is an open access article distributed under the terms and conditions of the Creative Commons Attribution (CC BY) license (<https://creativecommons.org/licenses/by/4.0/>).

typically comprises hydrogen storage tanks and a balance of plant (BoP) encompassing essential components such as fill ports, regulators, valves, and sensors.

Key concerns regarding the use of hydrogen as a marine fuel include its flammability range, potential for leakage, flame speed, and detonation/deflagration issues. Addressing these concerns necessitates specific studies to comprehend the associated risks and implement additional safeguards to prevent or mitigate major hazards, as documented in the literature [13,14].

The integration of hybrid powertrains, merging H<sub>2</sub> technologies with alternative energy sources and storage systems, presents a strategic avenue to enhance efficiency and circumvent the limitations inherent in standalone H<sub>2</sub> systems [15]. This integration facilitates a versatile and reliable power solution, highlighting the importance of investigating hybrid configurations in the pursuit of sustainable propulsion strategies for ships. Electric propulsion systems, while promising, entail a deep understanding of their advantages and limitations, for instance, related to the vessel designs, considering the risk analyses, and concerning the battery systems [16].

In this context, hydrogen FC technology emerges as a potential game-changer for marine transportation, offering a compelling alternative to traditional propulsion methods. Indeed, FC power systems are increasingly recognized as a pivotal option for enhancing the utilization of alternative marine fuels. Their remarkable energy efficiency renders them highly appealing when compared with traditional marine combustion engines and gas turbines. While it is acknowledged that FC power capacities may not currently meet the demands of all maritime applications, ongoing research and development efforts are focused on improving both the efficiency and power capabilities of FC power systems. This relentless pursuit of enhancement is steadily advancing the technology, inching it closer to widespread adoption each year [17,18]. However, the adoption of FC technology necessitates a comprehensive risk analysis encompassing the vessel design, operational considerations, and environmental impacts to ensure safe and effective operation.

The application of FCs in marine vessels dates back to the 1960s, particularly with their use on board underwater vehicles [19]. Merchant ships offer various potential applications for FCs, including providing low-power main propulsion, serving as auxiliary power sources for hybrid propulsion systems, generating electricity, and acting as emergency power supplies [20]. Notably, numerous demonstration projects showcasing fuel cell applications in the merchant marine sector have been conducted since the turn of the millennium [21]. Despite this, there have been only a few studies focusing on the utilization of H<sub>2</sub>-powered fuel cells for passenger ships [22,23]. Additionally, only a small number of demonstration boats [23–25] featuring proton-exchange membrane fuel cells (PEMs) with installed power capacities of up to 100 kW have been successfully tested for propulsion in both inland waters and the open sea. A literature review of existing studies on FCs for maritime applications revealed several key considerations: weight and volume, unit costs [26], safety and reliability analysis [27], and integration into hybrid systems for efficient solutions [25,28,29].

In this context, the contemporary approach to designing ships featuring innovative technologies, which are not covered by existing prescriptive rules, should adhere to the goal-based alternative design process, which involves the adoption of the “Equivalent Level of Safety” criteria [30]. The International Maritime Organization (IMO) endorsed interim guidelines for ships employing FC technologies and batteries during the 105th session of the Maritime Safety Committee (MSC) in April 2022 [31].

According to these statements, the present work aimed to investigate the performance of a hybrid powertrain, essentially consisting of a fuel cell system, a battery pack, and an electric motor, to be installed on board a catamaran ferry via the AVL Cruise-M simulation software (<https://www.avl.com/en/simulation-solutions/software-offering/simulation-tools-a-z/avl-cruise-m>, accessed on 29 April 2024). This study mainly focused on understanding the two energy sources’ responses to load variations and estimating the fuel consumption.

## 2. Case Study

The ship platform considered in the present work was the high-speed passenger ferry proposed in the feasibility study by Coppola et al. [32]. The passenger ferry is a full-electric catamaran equipped with a battery-assisted FC, with an overall length of 30 m and a beam of 10 m, and is designed to carry up to 220 passengers at a cruise speed of 20 kn. Table 1 presents the ferry's main characteristics, while Figure 1 shows the hull form and general appearance of the catamaran ferry.

**Table 1.** Main characteristics of the catamaran ferry.

Specification	Unit	Value
L <sub>OA</sub>	m	30
B <sub>OA</sub>	m	10
L <sub>WL</sub>	m	29.60
B	m	10
T	m	1.41
D	m	3.90
L <sub>CG</sub>	m	12.63
V <sub>CG</sub>	m	3.94
Displacement	t	125
Cruise speed	kn	20
Propulsion load	kW	1550
Hotel load	kW	30

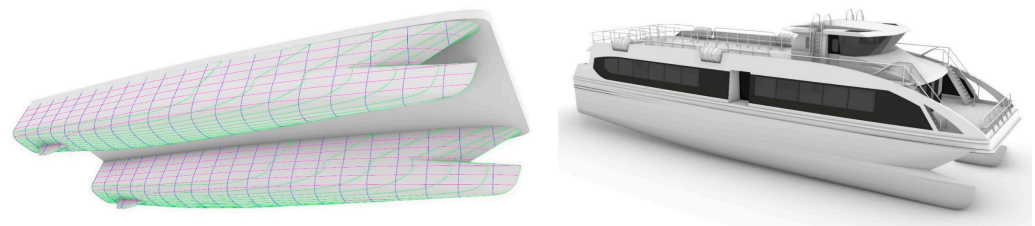


**Figure 1.** Hull form and appearance of the catamaran ferry.

The ferry provides a commuter service along the Amalfi Coast, conducting daily round trips from Salerno to Capri Island with several intermediate stops, with a laytime of 15 min. The duration of a single trip is approximately 3.28 h, assuming an average maneuvering time of 3 min.

The catamaran is designed to equip a fully electric propulsion plant system consisting of a couple of electric propulsion motors (EMs), one for each demi-hull, which move the propellers through the gearboxes and shafts. Such a plant is powered by an FC generating system made of PEM modules [33] and integrated with a battery system (BS).

A PEM basically converts the chemical energy of pure H<sub>2</sub> directly into electricity and heat, according to well-known reactions described in the literature [34]. The major advantages of a PEM include a high electrical efficiency (up to 65%), a low operating temperature (about 80 °C), a fast start-up (compared with other FC technologies), and a high-power density.

The BS is intended to assist the PEM in providing energy during transient operations, such as load demand variations, acceleration, and maneuvering phases [35]. In this study, we considered the lithium-ion batteries proposed by Zhang [36].

## 3. Simulation Model

The power plant propulsion system was modeled using the AVL Cruise-M software. AVL Cruise-M is a multidisciplinary vehicle system simulation tool for mobility concept analysis, subsystem design and layout, and virtual component integration [37]. The software allows the development of customized models with user-defined functions pro-

grammed in C. The implemented models used an object-oriented approach, capturing the components of each subsystem and their connections.

The subsequent section provides a short description of each model’s subsystems and units, which are shown in Figure 2.

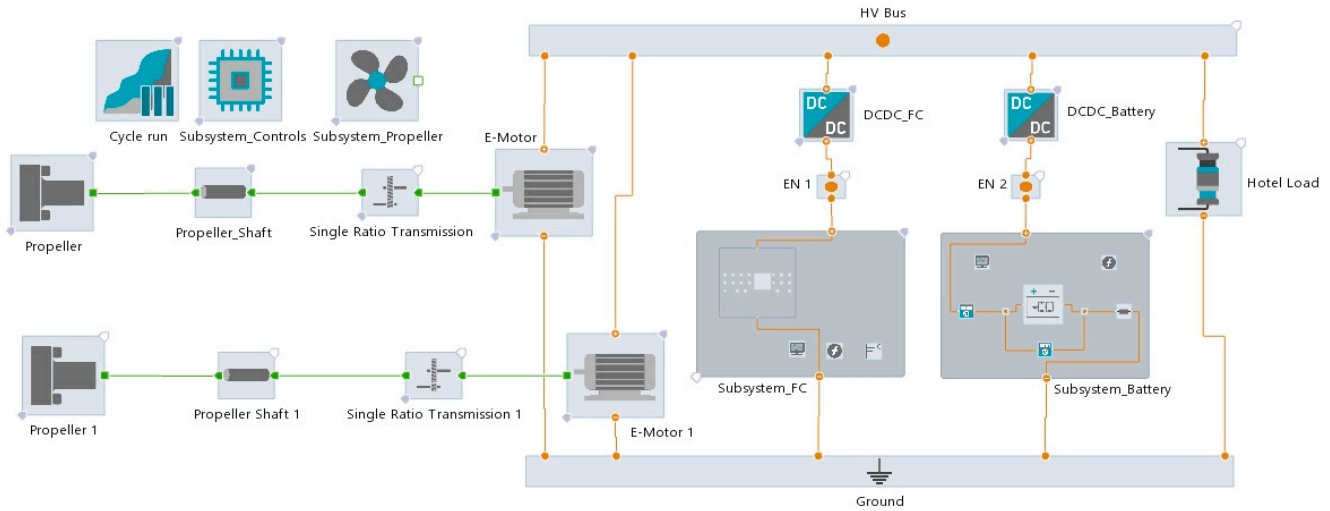


**Figure 2.** Block diagram of the full-electric powertrain for the catamaran demi-hull.

### 3.1. Hull and Propeller Subsystem

The hull and propeller subsystem (HPS) contains the ship’s resistance and the kinematics mathematical models. The hull characteristics are reported in Table 2. It is part of the new Naples Displacement Systematic Series (NDSS), currently under study at the Department of Industrial Engineering (DII) of Naples.

**Table 2.** Hull form’s principal dimensions.

Specification	Unit	Value
Hull		A 57 NDSS
LWL	m	24.79
BWL	m	4.52
T	m	141
Displacement	t	57

The hull performance, the total resistance ( $R_T$ ), and the effective power ( $P_E$ ) at the required speed were assessed by means of full-scale URANS simulations, considering a full-load condition of 125 t with the weight distribution calculated in [28]. The full-load displacement was estimated by referring to a database of similar ships [38]. The propulsive factors, the thrust deduction  $t$  and wake fraction  $w$  [39], and the appendage resistance (skeg, rudder, and shaft) were evaluated according to Holtrop and Mennen’s (1982) procedure [40]. Further details and the hypothesis adopted for these models have been described in detail in [41].

Considering the efficiencies and the propulsive factors, the total delivered power ( $P_D$ ) was calculated as:

$$P_D = P_E / \eta_D \tag{1}$$

where the propulsive efficiency ( $\eta_D$ ) can be expressed as the product of the hull efficiency ( $\eta_H$ ), propeller open-water efficiency ( $\eta_0$ ), and relative rotative efficiency ( $\eta_R$ ):

$$\eta_D = \eta_H \eta_0 \eta_R \tag{2}$$

where

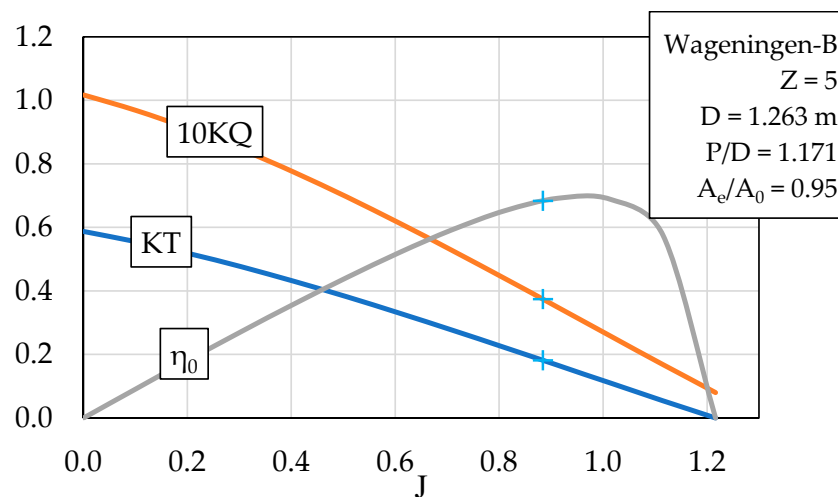
$$\eta_H = (1 - t) / (1 - w) \tag{3}$$

Table 3 reports the relevant performance data and efficiencies calculated at a design speed of 20 kn; further details are provided in [32].

**Table 3.** Ship performance data and efficiencies.

Specification	Unit	Value
Speed	kn	20
Total resistance	kN	74
Effective power	kW	761
$1 - t$	-	0.985
$1 - w$	-	0.965
$\eta_H$	-	1.021
$\eta_0$	-	0.68
$\eta_R$	-	1.00
Delivered power per axle	kW	545

Based on the estimated values of  $R_T$  and  $P_E$ , two 5-bladed Wageningen B propellers were selected with a diameter ( $D$ ) of 1.263 m, a pitch-to-diameter ( $P/D$ ) ratio of 1.171, and an expanded area-to-disc area ratio ( $A_e/A_0$ ) of 0.95. The propeller  $K_T$  and  $K_Q$  coefficient curves, the efficiency  $\eta_0$ , and the propeller working point are shown in the screw propeller open-water diagram reported in Figure 3.



**Figure 3.** Propeller open-water diagram of the selected propeller.

### 3.2. Electric Motor Subsystem

Based on the amount of power required to sail at the design speed, an appropriate EM and gearbox were selected. The electric motor subsystem (E-Motor; EMS) is characterized by torque and efficiency curves as a function of the voltage and speed, having a maximum efficiency value of 96% at 1600 rpm and 500 V, which corresponds to a torque of 4639 Nm and a mechanical power of 777 kW. These curves are shown in Figure 4.

The EMS drives the PS through a transmission and shaft unit and is connected to the main switchboard of the ship at 500 V.

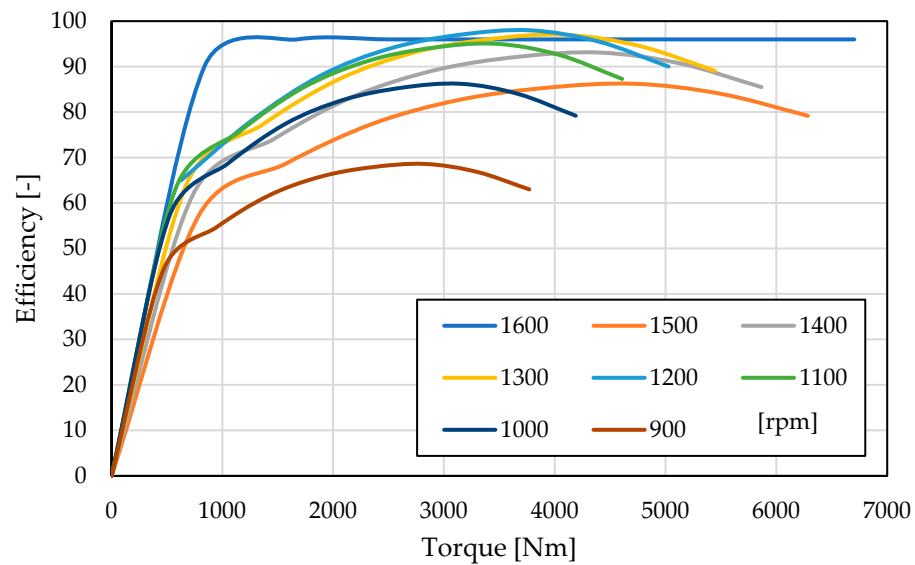


**Figure 4.** Electric motor efficiency–torque characteristic curves as a function of the rotation speed.

### 3.3. Fuel Cell Subsystem

The FC model separately accounts for the components of the PEM as well as all auxiliary devices and equipment (BoP), such as the cathode air supply, water and thermal management, power conditioning, etc. The model includes the following subsystems.

The FC stacks subsystem model features a 1D resolution along the gas channel flow and a reduced-dimensionality electrochemical model. The model comprises multiple cells with variable geometries, along with other physical and chemical specifics that users can customize or select from the software’s library. Users can also implement a single-cell performance (polarization curve). The FC stack model simulates the relevant thermodynamic, electrochemical, and transport processes occurring within the FC as a function of the components’ chosen materials.

The main specifications of the PEM stack are reported in Table 4, which includes average values taken from commercial products.

**Table 4.** Main specifications of the PEM stack.

Specification	Unit	Value
Rated power	kW	200
Min. power	kW	55
Peak efficiency	%	60
Operating temperature	°C	80
Operating voltage	V	350–720 DC
Weight	kg	1000
Dimensions	mm	1209 × 747 × 2195

The anode subsystem (AS) models the H<sub>2</sub> flow in the anode FC section, including a recirculation branch of unused humid hydrogen that is fed back through a Venturi injector. Excess water from the anode gas outflow is removed by a water separator to maintain a constant humidity. A PID is used to control the Venturi injector opening and regulate the pressure. The AS also contains the H<sub>2</sub> tank subsystem, which is made of a tank plenum supplemented with a charging valve restriction, a discharging valve restriction, a relief device valve restriction, and a relief device control function.

The cathode subsystem consists of a compressor, which can provide up to ~0.5 kg/s of external air pumped up to 4 bar. The compressed air is cooled down and then circulated through the humidifier component before reaching the FC stack to provide the desired

humidity to the membrane. The pressure and airflow are regulated via two PID controllers that control the compressor and the backpressure valve.

The thermal management subsystem (TMS) simulates a cooling circuit that uses environmental water to exchange heat. Circulation in the TMS is driven by a pump that is regulated considering the heat flow generated by the FC system with a correction provided by a PID to maintain the FC temperature at a constant value of 80 °C.

Block diagrams of the PEM subsystems are presented in Figure 5.

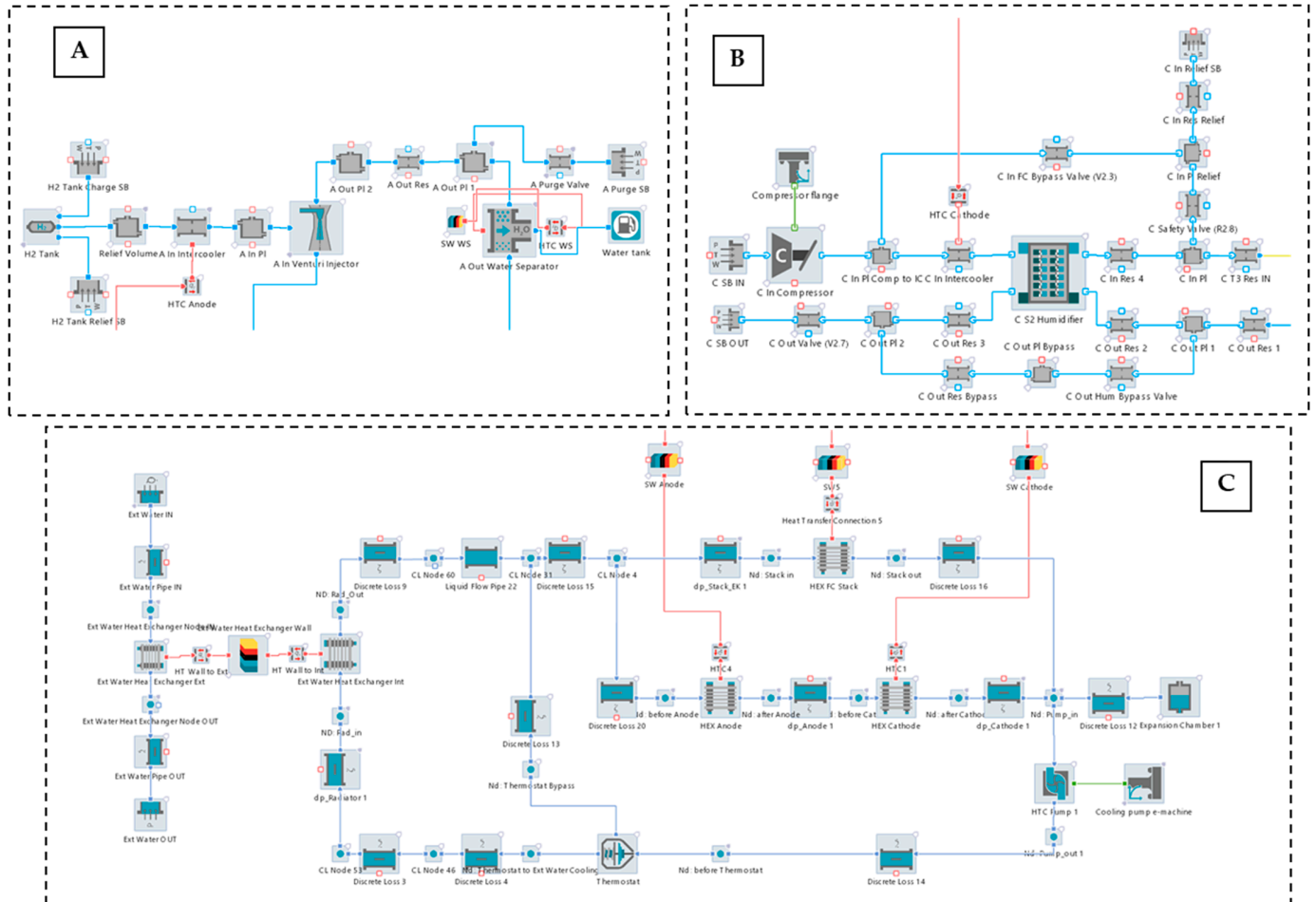


**Figure 5.** Block diagrams of the PEM subsystems: (A) anode subsystem, (B) cathode subsystem, and (C) thermal management subsystem.

### 3.4. Battery Subsystem

The battery subsystem (BS) consists of a controlled voltage source and an ohmic resistance, which is used to describe the instantaneous voltage response to a current input. It includes an advanced model to predict the transient voltage response to a dynamic current load, eventually coupled with a thermal model to predict the transient thermal behavior of the battery. The BS is made of battery packs consisting of multiple cells connected in series and parallel with a battery management system (BMS) for peak and continuous power. It serves as recuperation storage, as a buffer when the FC system is active, and as the main storage when the power request is below the activation threshold of the FC system.

The battery system must be specifically designed according to the case study ship and operating routing profile, for instance, varying the initial state of charge (SoC), the operating voltage, and the single-cell configuration (series–parallel). Open-circuit voltage

and ohmic resistance variations as a function of the SoC were implemented, assuming the trend for lithium-ion batteries at 25 °C presented by Zhang and shown in Figure 6 [36].

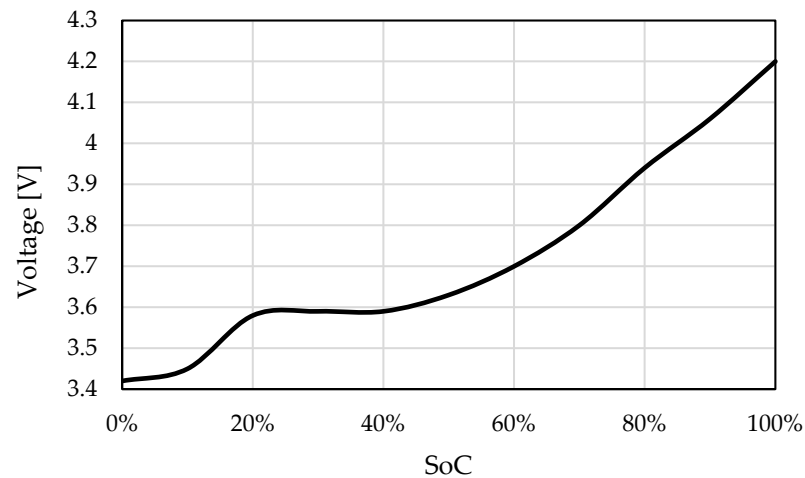


**Figure 6.** Open-circuit voltage and ohmic resistance variations as a function of the SoC.

During normal operation, the battery is assumed to be charged to approximately 90% of the SoC, with the minimum expected SoC being at least 30%. If the power demand rises too quickly or goes above the maximum rated power of the FC subsystem, the battery covers for the remainder.

As the EM, FC stacks, and BS operate within different voltage ranges, two DC–DC converter units are considered to boost the voltages up to the EM side level. Both DC–DC converters have an estimated efficiency of 93%.

### 3.5. Operating Routing Profile and Experimental Validation

The performance of the powertrain system was analyzed considering the operating routing profile shown in Figure 7. This profile assumes a 15 min operating period, consisting of a constant cruise speed of 20 knots and a maneuvering phase, including acceleration and deceleration, with an almost linear trend lasting for 3 min.

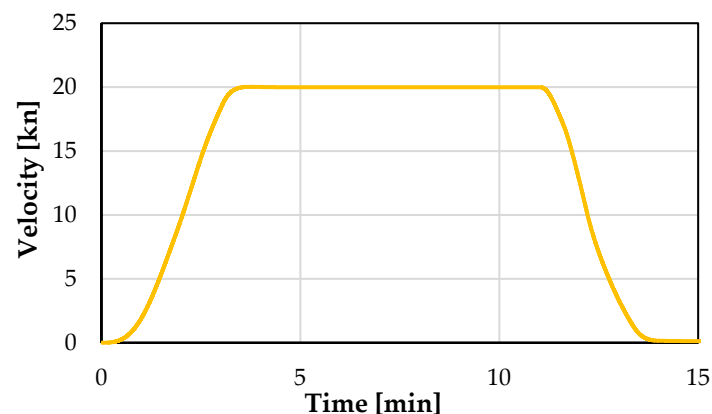


**Figure 7.** Ship velocity profile.

It should be emphasized that in the catamaran, there are two separate and identically powered generators, each accounting for half of the overall power needed by the ship, which are in each demi-hull and equipped with a propeller powertrain system. Despite the scheme in Figure 2 showing two EM subsystems and singular FC and BS subsystems, simulation tests were conducted for a single powertrain, and the results are presented accordingly.

Considering that every element in the software's models has been validated and verified by experts and other authors in the literature [42–44], experimental validation of the model in the present work was not strictly necessary. The primary objective of this investigation was to determine the power requirements of each component and to predict the preliminary performance of the powertrain system mainly during the maneuvering phase (under dynamic conditions).

#### 4. Results

Preliminary tests were undertaken to meticulously fine-tune the power size of every component within the powertrain system. This comprehensive optimization process encompassed not only the configuration of both the fuel cell (FC) and battery system (BS) but also delved into aspects such as the number of stacks and their arrangement. Special attention was dedicated to optimizing the installed battery capacity, recognizing its pivotal role in influencing the overall design of the ship. It was acknowledged that these parameters could significantly impact the ship's design, particularly in terms of excessive embarked weights and volumes.

Upon evaluating the requirements for a round trip, it was determined that the power-generating system needed to consist of a fuel cell comprising eight stacks delivering a maximum power output of 1600 kW, and a BS with an installed capacity of approximately 2 kWh.

Figure 8A illustrates the variations in the FC and BS power responses corresponding to the total load demand depicted in the operating routing profile in Figure 7. The load demand primarily comprises two EM power requests and the hotel load, with the latter assumed to remain constant at 30 kW. Essentially, the electric system operates as follows: When the electrical power demand applied to the electrical network in the powertrain by the EM exceeds the electric energy supplied by the FC (or its activation threshold value), the power demand is met by the BS. Conversely, when the power demand is lower than the FC supply, the surplus energy charges the BS up to a SoC of 90%. Subsequently, the FC will reduce the power production. According to Figure 8B, the BS is active during the maneuvering phase, especially during the acceleration from 0 to 20 knots. Figure 8B also illustrates the behavior of the electric system during the start-up phase. In this scenario, the fuel cell is assumed to be in a standby condition, maintaining an operating temperature of 80 °C, with the polymeric electrolyte membrane already humidified. Additionally, there is an immediate step load demand of 30 kW due to the hotel's load and the initial power request of the electric motor, which is approximately 100 kW. In this case, the presence of the BS ensures the power demand with a fast response (<0.5 s), allowing the FC to reach the operating condition within about 6 sec. After approximately 3 min, when the total load demand exceeds its peak, the FC begins charging the battery system to restore the battery's SoC. Consequently, the FC generates approximately 749.9 kW for about 1.6 min after each acceleration to 20 knots, for each powertrain. This charging persists even if the EM power demand decreases, eventually reaching a steady value of 714.5 kW.

The calculated FC's efficiency in cruising mode is about 59.5%, while during load variations (maneuvering phase) and with a very low power supply, the FC's efficiency could briefly reach values as low as about 20%.

The estimation of the BS's capacity was based on the results presented in Figure 8B: it considered the area of the BS plot (positive values) from 0 to approximately 1.4 min, yielding a value of about 1.2 kWh. Taking into account the battery's SoC variation between 90% and 30%, the total required capacity is approximately 2 kWh. It should be noted that this value only corresponds to the specific energy demand (or power profile) derived from the required ship velocity profile shown in Figure 7 and may not necessarily represent the final installed battery capacity, which should consider a more complex power profile and redundancy factor, among other things.

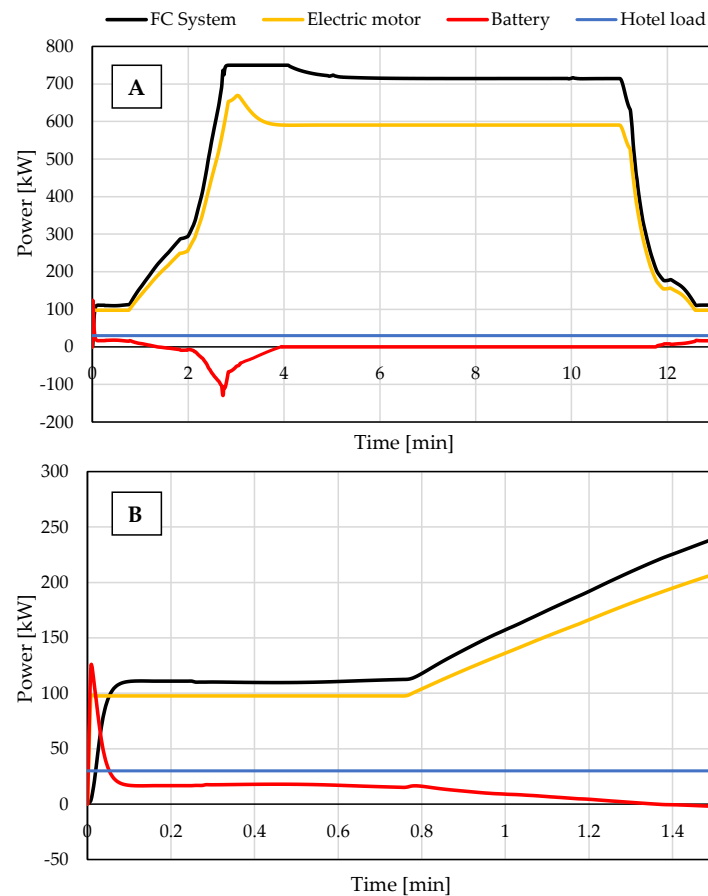


**Figure 8.** (A) Power variation over the routing profile for the electric motor, hotel load, fuel cell, and battery; (B) details of the battery and fuel cell systems' behaviors during the start-up phase.

An estimation of the overall  $H_2$  required for a round trip (Salerno–Capri Island) was also conducted. Specifically, it was found that the total amount of  $H_2$  to be stored on board is about 250 kg, with an average  $H_2$  flow rate consumption of  $3.5 \text{ kg}_{H_2}/\text{nm}$ . In order to accommodate the storage of  $H_2$  on board the catamaran ferry, the utilization of cylindrical type IV tanks operating at a 700 bar pressure was considered. This would necessitate the procurement of eight such vessels to meet the storage requirements. These tanks would collectively occupy an estimated volume of  $9.5 \text{ m}^3$  and have a combined weight of 3.2 tons. These calculations are based on the average values derived from the gravimetric and volumetric densities of commercially available products. It should be noted that an additional cylindrical tank should be considered as a precautionary measure.

## 5. Conclusions

This paper highlights the importance of sustainability in the maritime sector and the potential of hydrogen as an alternative fuel. In this study, a fully electric powertrain was designed and analyzed for a high-speed passenger catamaran ferry. For this purpose, the powertrain was mathematically modeled using the AVL Cruise-M software for a specific route (Salerno–Capri Island) and a cruise speed of 20 knots. Simulation tests were conducted to determine the power size of the main components of the powertrain, which essentially included a fuel cell system (1600 kW), a battery system (2 kWh), and an electric motor ( $2 \times 777 \text{ kW}$ ), and to estimate the hydrogen consumption ( $3.5 \text{ kg}_{H_2}/\text{nm}$ ) and the amount of hydrogen to be stored on board for a round trip (250 kg). It was assumed that the hydrogen would be stored in nine type IV cylindrical vessels at 700 bar, located externally on the upper deck.

The results show the need for an energy storage system alongside the FC generating system to assist during high load variations. Meanwhile, the required battery capacity is very low, not involving any particular issues for installation on board. Integrating hybrid powertrains into marine propulsion systems is a strategy to enhance the overall performance and energy economy of these ships.

Future work will focus on conducting a detailed assessment of EM propulsion efficiencies and weight optimization, including structures and general arrangements. This effort will aim to enhance the project design process by reducing uncertainties. Additionally, these studies will consider the regulatory framework and how the proposed system addresses compliance requirements.

This approach to studying hybrid propulsion systems has broader applicability beyond the specific case study of the catamaran ferry. The insights gained from our research can inform the design and operation of hybrid powertrains in other maritime settings and, potentially, other transportation sectors as well.

**Author Contributions:** Conceptualization, L.M., R.R. and T.C.; methodology, L.M.; software, L.M. and R.R.; validation, L.M.; formal analysis, L.M.; investigation, L.M., R.R. and V.S.; resources, L.M.; data curation, L.M., R.R. and V.S.; writing—original draft preparation, L.M. and R.R.; writing—review and editing, L.M. and R.R.; visualization, L.M.; supervision, L.M. and T.C.; project administration, L.M.; funding acquisition, L.M. All authors have read and agreed to the published version of the manuscript.

**Funding:** This research received no external funding.

**Institutional Review Board Statement:** Not applicable.

**Informed Consent Statement:** Not applicable.

**Data Availability Statement:** No new data were created or analyzed in this study. Data sharing is not applicable to this article.

**Conflicts of Interest:** The authors declare no conflicts of interest.

## References

1. McCarthy, J.E. Air Pollution and Greenhouse Gas Emissions from Ships. Available online: [https://www.researchgate.net/publication/292369655\\_Air\\_pollution\\_and\\_greenhouse\\_gas\\_emissions\\_from\\_ships](https://www.researchgate.net/publication/292369655_Air_pollution_and_greenhouse_gas_emissions_from_ships) (accessed on 18 March 2024).
2. Huang, D.; Wang, Y.; Yin, C. Selection of CO<sub>2</sub> Emission Reduction Measures Affecting the Maximum Annual Income of a Container Ship. *J. Mar. Sci. Eng.* **2023**, *11*, 534. [CrossRef]
3. Tarhan, C.; Çil, M.A. A Study on Hydrogen, the Clean Energy of the Future: Hydrogen Storage Methods. *J. Energy Storage* **2021**, *40*, 102676–102686. [CrossRef]
4. DNV Ammonia as a Marine Fuel. Available online: <https://www.dnv.com/publications/ammonia-as-a-marine-fuel-191385/> (accessed on 18 March 2024).
5. American Bureau of Shipping (ABS). *Sustainability-Methanol-as-Marine-Fuel*; ABS: Spring, TX, USA, 2021; pp. 1–24.
6. Ahbabi Saray, J.; Gharehghani, A.; Hosseinzadeh, D. Towards Sustainable Energy Carriers: A Solar and Wind-Based Systems for Green Liquid Hydrogen and Ammonia Production. *Energy Convers. Manag.* **2024**, *304*, 118215. [CrossRef]
7. Inal, O.B.; Zincir, B.; Deniz, C. Investigation on the Decarbonization of Shipping: An Approach to Hydrogen and Ammonia. *Int. J. Hydrogen Energy* **2022**, *47*, 19888–19900. [CrossRef]
8. Kumar Singla, M.; Nijhawan, P.; Singh Oberoi, A. Hydrogen Fuel and Fuel Cell Technology for Cleaner Future: A Review. *Environ. Sci. Pollut. Res. Int.* **2021**, *28*, 15607–15626. [CrossRef]
9. van Biert, L.; Godjevac, M.; Visser, K.; Aravind, P.V. A Review of Fuel Cell Systems for Maritime Applications. *J. Power Sources* **2016**, *327*, 345–364. [CrossRef]
10. Bosu, S.; Rajamohan, N. Recent Advancements in Hydrogen Storage—Comparative Review on Methods, Operating Conditions and Challenges. *Int. J. Hydrogen Energy* **2023**, *52*, 352–370. [CrossRef]
11. Lai, Q.; Paskevicius, M.; Sheppard, D.A.; Buckley, C.E.; Thornton, A.W.; Hill, M.R.; Gu, Q.; Mao, J.; Huang, Z.; Hua, L.; et al. Hydrogen Storage Materials for Mobile and Stationary Applications: Current State of the Art. *ChemSusChem* **2015**, *8*, 2789–2825. [CrossRef]
12. Shin, H.K.; Ha, S.K. A Review on the Cost Analysis of Hydrogen Gas Storage Tanks for Fuel Cell Vehicles. *Energies* **2023**, *16*, 5233. [CrossRef]

13. International Maritime Organization (IMO) IGF Code. Available online: <https://www.imo.org/en/ourwork/safety/pages/igf-code.aspx> (accessed on 13 March 2024).
14. Dolci, F.; Jordan, T.; Keller, J.; e Moretto, P. Research Priority Workshop on Hydrogen Safety. Publications Office of the European Union: Luxembourg, 2018. [CrossRef]
15. Ma, S.; Lin, M.; Lin, T.E.; Lan, T.; Liao, X.; Maréchal, F.; Van herle, J.; Yang, Y.; Dong, C.; Wang, L. Fuel Cell-Battery Hybrid Systems for Mobility and off-Grid Applications: A Review. *Renew. Sustain. Energy Rev.* **2021**, *135*, 110119. [CrossRef]
16. Samsun, R.C.; Krupp, C.; Baltzer, S.; Gnörich, B.; Peters, R.; Stolten, D. A Battery-Fuel Cell Hybrid Auxiliary Power Unit for Trucks: Analysis of Direct and Indirect Hybrid Configurations. *Energy Convers. Manag.* **2016**, *127*, 312–323. [CrossRef]
17. Ferrari, M.L.; Traverso, A.; Massardo, A.F. Smart Polygeneration Grids: Experimental Performance Curves of Different Prime Movers. *Appl. Energy* **2016**, *162*, 622–630. [CrossRef]
18. Xing, H.; Stuart, C.; Spence, S.; Chen, H. Fuel Cell Power Systems for Maritime Applications: Progress and Perspectives. *Sustainability* **2021**, *13*, 1213. [CrossRef]
19. McConnell, V.P. Now, Voyager? The Increasing Marine Use of Fuel Cells. *Fuel Cells Bulletin* **2010**, *2010*, 12–17. [CrossRef]
20. Sattler, G. Fuel Cells Going On-Board. *J. Power Sources* **2000**, *86*, 61–67. [CrossRef]
21. Tronstad, T.; Åstrand, H.H.; Haugom, G.P.; Langfeldt, L. *Study on the Use of Fuel Cells in Shipping*; EMSA European Maritime Safety Agency: Oslo, Norway, 2017.
22. Ahn, J.; Noh, Y.; Joung, T.; Lim, Y.; Kim, J.; Seo, Y.; Chang, D. Safety Integrity Level (SIL) Determination for a Maritime Fuel Cell System as Electric Propulsion in Accordance with IEC 61511. *Int. J. Hydrogen Energy* **2019**, *44*, 3185–3194. [CrossRef]
23. Ahn, J.; Noh, Y.; Park, S.H.; Choi, B.I.; Chang, D. Fuzzy-Based Failure Mode and Effect Analysis (FMEA) of a Hybrid Molten Carbonate Fuel Cell (MCFC) and Gas Turbine System for Marine Propulsion. *J. Power Sources* **2017**, *364*, 226–233. [CrossRef]
24. Jeon, H.; Park, K.; Kim, J. Comparison and Verification of Reliability Assessment Techniques for Fuel Cell-Based Hybrid Power System for Ships. *J. Mar. Sci. Eng.* **2020**, *8*, 74. [CrossRef]
25. Choi, C.H.; Yu, S.; Han, I.S.; Kho, B.K.; Kang, D.G.; Lee, H.Y.; Seo, M.S.; Kong, J.W.; Kim, G.; Ahn, J.W.; et al. Development and Demonstration of PEM Fuel-Cell-Battery Hybrid System for Propulsion of Tourist Boat. *Int. J. Hydrogen Energy* **2016**, *41*, 3591–3599. [CrossRef]
26. Leo, T.J.; Durango, J.A.; Navarro, E. Exergy Analysis of PEM Fuel Cells for Marine Applications. *Energy* **2010**, *35*, 1164–1171. [CrossRef]
27. Sasank, B.V.; Rajalakshmi, N.; Dhathathreyan, K.S. Performance Analysis of Polymer Electrolyte Membrane (PEM) Fuel Cell Stack Operated under Marine Environmental Conditions. *J. Mar. Sci. Technol.* **2016**, *21*, 471–478. [CrossRef]
28. Wang, Z.; Dong, B.; Yin, J.; Li, M.; Ji, Y.; Han, F. Towards a marine green power system architecture: Integrating hydrogen and ammonia as zero-carbon fuels for sustainable shipping. *Int. J. Hydrogen Energy* **2024**, *50*, 1069–1087. [CrossRef]
29. Jeong, J.; Seo, S.; You, H.; Chang, D. Comparative Analysis of a Hybrid Propulsion Using LNG-LH2 Complying with Regulations on Emissions. *Int. J. Hydrogen Energy* **2018**, *43*, 3809–3821. [CrossRef]
30. *MSC.1/Circ. 1455*; Guidelines for the Approval of Alternatives and Equivalent as Provided for in Various Imo Instruments. IMO: London, UK, 2013.
31. *MSC.1/Circ. 1647*; Annex Interim Guidelines for the Safety of Ships Using Fuel Cell Power Installations. IMO: London, UK, 2022.
32. Coppola, T.; De Luca, F.; Gambardella, S.; Mancini, S.; Micoli, L.; Pensa, C.; Sorrentino, V. Feasibility Study of a Zero-Emission Passenger Catamaran Ferry Operating in Italian Coastal Island. In Proceedings of the Progress in Marine Science and Technology, Naples, Italy, 23–25 October 2023; Volume 7, pp. 172–180.
33. Ballard Ballard. Available online: <https://www.ballard.com/> (accessed on 29 January 2024).
34. Yuan, X.Z.; Wang, H. *PEM Fuel Cell Electrocatalysts and Catalyst Layers*; Zhang, J.J., Ed.; Springer: London, UK, 2008.
35. Truong, H.V.A.; Dao, H.V.; Do, T.C.; Ho, C.M.; To, X.D.; Dang, T.D.; Ahn, K.K. Mapping Fuzzy Energy Management Strategy for PEM Fuel Cell–Battery–Supercapacitor Hybrid Excavator. *Energies* **2020**, *13*, 3387. [CrossRef]
36. Zhang, R.; Xia, B.; Li, B.; Cao, L.; Lai, Y.; Zheng, W.; Wang, H.; Wang, W.; Wang, M. A Study on the Open Circuit Voltage and State of Charge Characterization of High Capacity Lithium-Ion Battery Under Different Temperature. *Energies* **2018**, *11*, 2408. [CrossRef]
37. AVL. Available online: <https://www.avl.com/en> (accessed on 29 January 2024).
38. Fang, S.; Liu, Z.; Wang, X.; Cao, Y.; Yang, Z. Dynamic Analysis of Emergency Evacuation in a Rolling Passenger Ship Using a Two-Layer Social Force Model. *Expert Syst. Appl.* **2024**, *247*, 123310. [CrossRef]
39. Miranda, S. Architettura Navale. Available online: <http://www.liguori.it/schedanew.asp?isbn=5255> (accessed on 30 March 2024).
40. Holtrop, J.; Mennen, G.G.J. *An Approximate Power Prediction Method*; International Shipbuilding Progress: Amsterdam, The Netherlands, 1982; pp. 166–170.
41. Sorrentino, V.; Altosole, M.; De Luca, F.; Micoli, L.; Mocerino, L.; Russo, R. Preliminary Modeling of a Ferry Methanol Fuel Cell Power Plant by Using AVL Cruise M Software. In Proceedings of the Developments in Maritime Technology and Engineering—Proceedings of the 7th International Conference on Maritime Technology and Engineering, MARTECH 2024; Soares, C.G., Santos, T.A., Eds.; CRC Press/Balkema: Lisbon, Portugal, 2024.
42. Salek, F.; Abouelkhair, E.; Babaie, M.; Cunliffe, F.; Nock, W. *Multi-Objective Optimization of the Fuel Cell Hybrid Electric Powertrain for a Class 8 Heavy-Duty Truck*; SAE International: Warrendale, PA, USA, 2023. [CrossRef]

43. Liu, M.; Li, Y.; Xu, L.; Wang, Y.; Zhao, J. General Modeling and Energy Management Optimization for the Fuel Cell Electric Tractor with Mechanical Shunt Type. *Comput. Electron. Agric.* **2023**, *213*, 108178. [[CrossRef](#)]
44. Wancura, H.; Kühberger, G.; Schutting, E. Concept Evaluation of a P2 MHEV SUV: Application for Possible EU7 Boundaries. *Automot. Engine Technol.* **2023**, *8*, 1–16. [[CrossRef](#)]

**Disclaimer/Publisher’s Note:** The statements, opinions and data contained in all publications are solely those of the individual author(s) and contributor(s) and not of MDPI and/or the editor(s). MDPI and/or the editor(s) disclaim responsibility for any injury to people or property resulting from any ideas, methods, instructions or products referred to in the content.